iScience, Volume *27*

Supplemental information

Layer specific regulation of critical period timing and maturation of mouse visual cortex by endocannabinoids

Taisuke Yoneda, Katsuro Kameyama, Takahiro Gotou, Keiko Terata, Masahiro Takagi, Yumiko Yoshimura, Kenji Sakimura, Masanobu Kano, and Yoshio Hata

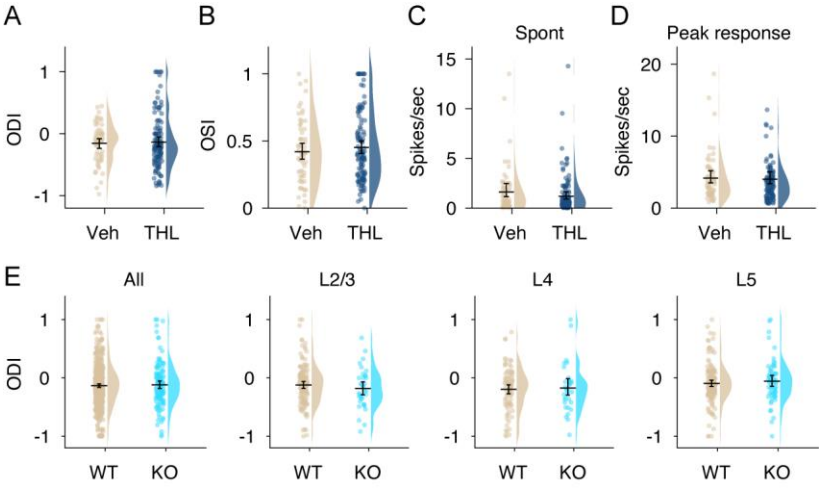

Figure S1. Visual response properties of V1 neurons in THL-treated mice and DGLα-KO mice, related to Figure 1. (A–D) Various characteristics of neuronal activity in THL- or vehicle-treated V1. THL or vehicle solution was continuously infused to V1 of P30 wild-type mice for 1–2 days. THL treatment does not affect the distribution of ODI (A) (P = 0.780, g = 0.044), OSI (B) (P = 0.430, g = 0.124), spontaneous spikes (C) (P = 0.189, g = 0.211), and peak responses (D) (P = 0.809, g = 0.039) (Veh; n = 61 units from 2 mice, THL; n = 119 units from 3 mice). (E) Raincloud plots show the OD distribution in all cortical layers (All) of nondeprived wild-type (WT, the same data as WT in Figure 1) and age-matched DGLα-KO mice (KO, n = 128 units in 2 mice), together with their layer breakdown (KO, n = 35 (L2/3), 33 (L4), and 60 (L5)). Lack of DGLα does not affect OD distribution (All, P = 0.699, g = 0.039; L2/3, P = 0.379, g = 0.167; L4, P = 0.764, g = 0.061; L5, P = 0.467, g = 0.111). Permutation test was performed.

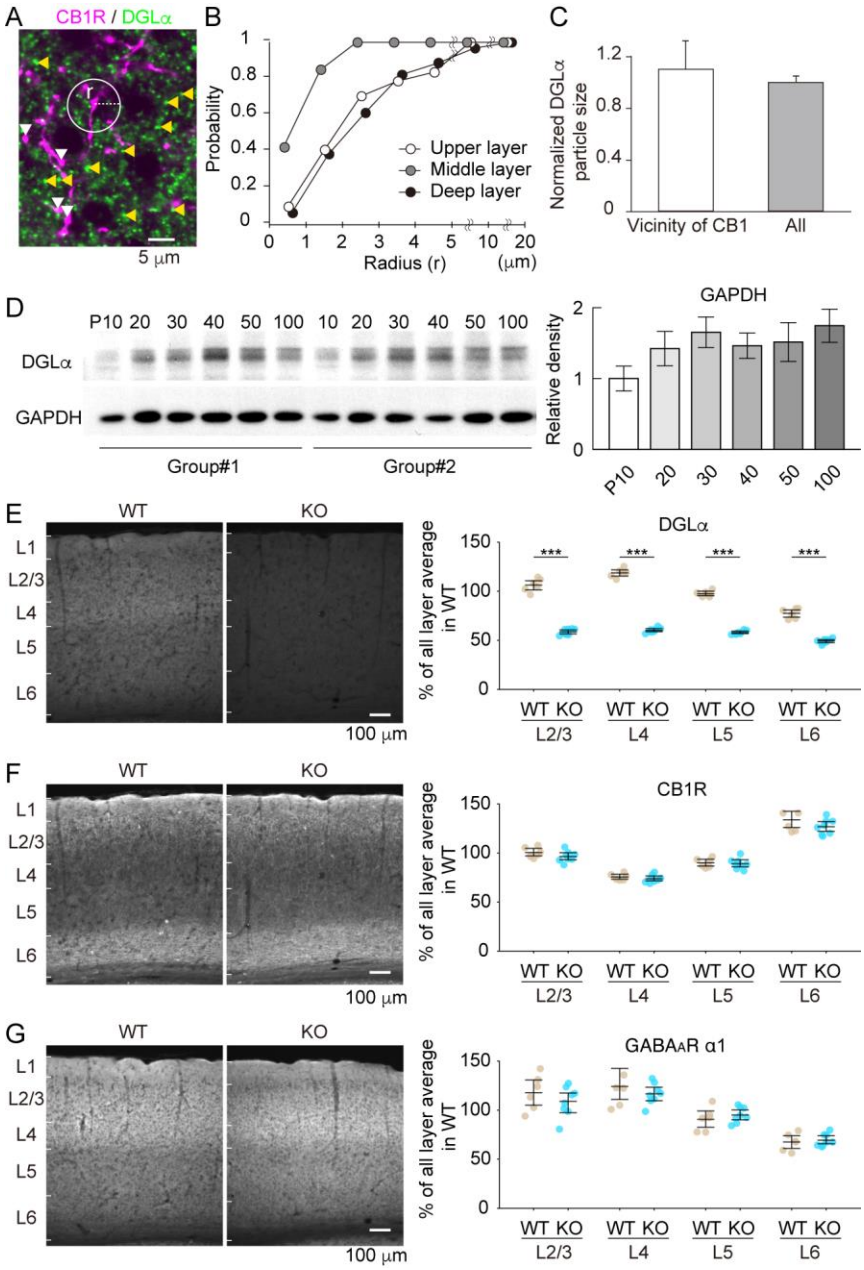

Figure S2. Expression of DGLα, CB1R, and GABA$_A$R in wild-type and DGLα-KO mice, related to Figure 3. (A) Double immunofluorescence staining of DGLα (green) and CB1R (magenta) in the upper layer of the V1 binocular region of wild-type mice. White and yellow arrowheads indicate CB1R-immunopositive boutons and DGLα-immunopositive particles, respectively. The white circle represents an example of ROI used for evaluating the number of DGLα particles around the CB1R bouton. (B) Cumulative distribution of the existence probability of DGLα particles at various distances from CB1R boutons in the upper, middle, and deep layers. (C) The size of DGLα particles within 1 μm around CB1R boutons (Vicinity of CB1, *n* = 28) and the size of all DGLα particles (All, *n* = 2078). The size was normalized to the mean size of all DGLα particles

(error bars, SEM). Distance between DGLα particles and CB1R boutons does not correlate with the size of DGLα particles (unpaired *t*-test, $P > 0.05$). (D) Example of western blots different from Figure 3D showing DGLα and GAPDH expression in V1 of wild-type mice at various postnatal ages. Two different sample groups taken from animals at various ages were loaded on one gel. In the graph on the right, relative densities of western blot bands for GAPDH are plotted at various ages (n = 10 hemispheres in 5 mice for each age; bars, mean; error bars, SEM). Band densities are normalized to the density at P10 (one-way ANOVA, $P > 0.05$). (E–G) Representative image of immunostained for DGLα (E), CB1R (F), and $GABA_AR$ α1 (G) in wild-type and DGLα-KO mice. In the graph on the right, intensity profiles in individual layers are shown. The intensity in each layer is normalized to the all-layer average of wild type (*n* = 6 ROIs in 3 mice for WT; *n* = 8 ROIs in 4 mice for KO). The black horizontal bar and error bars indicate mean and 95% CI, respectively. Permutation test was performed (***$P < 0.001$).

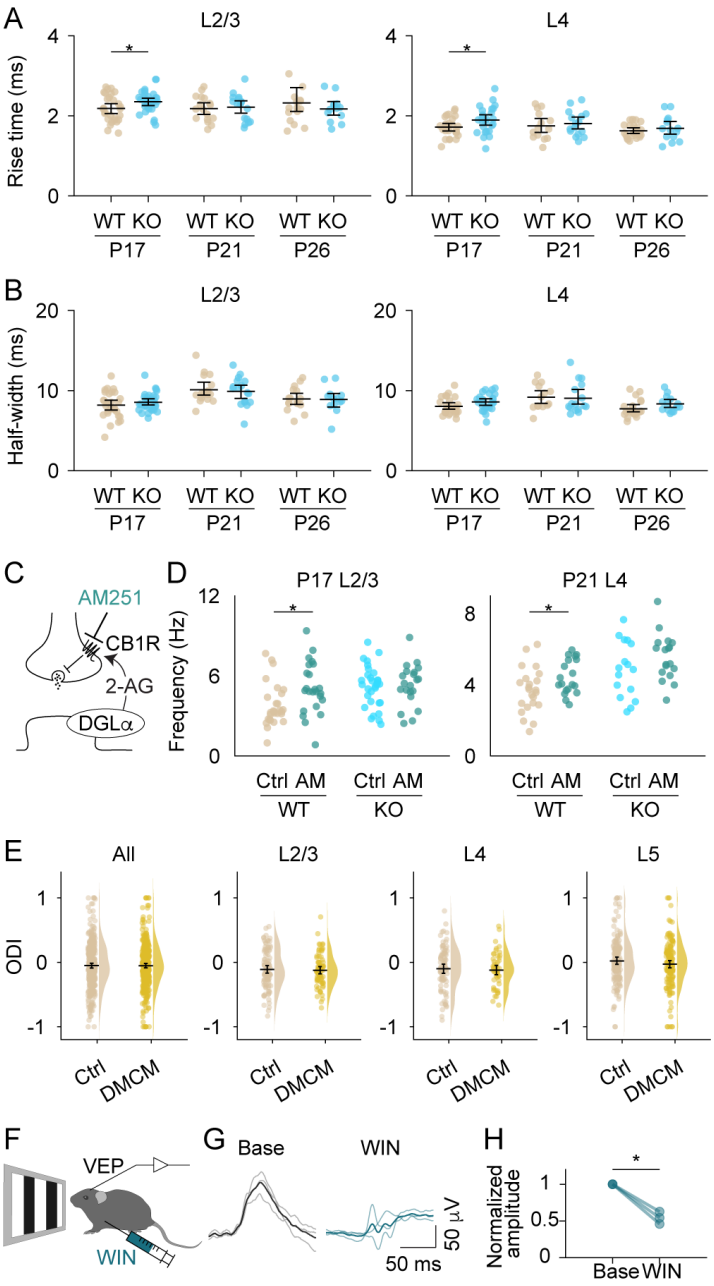

Figure S3. mIPSC kinetics in DGLα-KO mice and effects of various pharmacological manipulations in vitro and in vivo, related to Figure 4. (A and B) Rise time (A) and half-width (B) of mIPSCs recorded from pyramidal neurons in L2/3 (WT, *n* = 28 (P17), 17 (P21), and 16 (P26) cells; KO, *n* = 31 (P17), 17 (P21), and 13 (P26) cells) and in L4 (WT, *n* = 25 (P17), 23 (P21), and 21 (P26) cells; KO, *n*= 25 (P17), 16 (P21), and 14 (P26) cells). Colored circles show data from individual cells. The black horizontal bar and error bars indicate mean and 95% CI, respectively. DGLα-KO mice showed significantly longer rise time at P17 (L2/3; P17, $P < 0.05$, $g = 0.550$; P21, $P = 0.744$, $g = 0.109$, P26, $P = 0.458$, $g = 0.306$, L4; P17, $P < 0.05$, $g = 0.598$, P21, $P = 0.888$, $g =$

0.044, P26, $P = 0.473$, $g = 0.251$). Half-width of mIPSCs was comparable with that of WT mice (L2/3; P17, $P = 0.346$, $g = 0.250$, P21, $P = 0.741$, $g = 0.116$, P26, $P = 0.897$, $g = 0.050$, L4; P17, $P = 0.067$, $g = 0.522$, P21, $P = 0.674$, $g = 0.142$, P26, $P = 0.106$, $g = 0.575$). (C) AM251 (AM), a CB1R inverse agonist was bath-applied to block CB1R during whole-cell patch-clamp recording in mouse V1 slices. (D) mIPSC frequency of pyramidal neurons in L2/3 of P17 mice (AM WT, $n = 24$ and AM KO, $n = 21$ cells) and L4 of P21 mice (AM WT, $n = 19$ and AM KO, $n = 18$ cells). The data for control animals are the same as in Figure 4C. In both cases, bath-application of AM251 significantly increased mIPSC frequency in wild-type mice (P17 L2/3 WT, $P < 0.05$, $g = 0.745$; P21 L4 WT, $P < 0.05$, $g = 0.680$) but not in DGLα-KO mice (P17 L2/3 KO, $P = 0.751$, $g = 0.090$; P21 L4 KO, $P = 0.172$, $g = 0.486$). (E) Raincloud plots show the OD distribution in each layer of nondeprived P21 WT mice (Ctrl, the same data as P21 WT in Figure 2A) and DMCM treated nondeprived P21 DGLα-KO mice (DMCM, $n = 376$ (All layer), 77 (L2/3), 51 (L4), and 159 (L5) units in 5 mice). DMCM does not affect OD distribution (All, $P = 0.916$, $g = 0.008$; L2/3, $P = 0.718$, $g = 0.057$; L4, $P = 0.676$, $g = 0.073$; L5, $P = 0.221$, $g = 0.140$). (F) We recorded VEP in V1 of wild-type mice before and after the intraperitoneal administration of WIN. (G) Traces of VEP before (Base) and 1 hour after WIN administration. Thin traces represent the average trace of 500 times of VEPs recorded in individual animals and thick traces represent the mean of all animals. (H) The mean amplitude of VEP of each animal. The amplitude is normalized to that of Base in each animal. WIN administration induced a significant reduction in VEP amplitude ($P < 0.05$, $g = 2.800$, 3 mice). Permutation test was conducted in (A), (B), (D) and (E), and paired *t*-test was performed in (H) (*$P < 0.05$).

Table S1. Summary of experimental conditions and statistics, related to Figures 1, 2, and 4.

Cohort	Age	Layer	n (animals)	n(cells)	Parameter	mean	SEM	95% CI		Figure
WT_noMD	P31-34	all	12	530	ODI	-0.134	0.015	-0.164	-0.103	1
WT_VehMD	P31-34	all	4	153	ODI	0.045	0.035	-0.020	0.115	1
WT_THLMD	P31-34	all	4	161	ODI	-0.100	0.033	-0.163	-0.032	1
WT_MD	P31-34	all	6	259	ODI	0.181	0.027	0.129	0.234	1
DGLαKO_MD	P31-34	all	7	261	ODI	-0.020	0.025	-0.069	0.028	1
DGLβKO_MD	P31-34	all	4	124	ODI	0.118	0.035	0.047	0.182	1
WT_noMD	P31-34	L2/3	9	140	ODI	-0.123	0.030	-0.178	-0.064	1
WT_MD	P31-34	L2/3	6	87	ODI	0.195	0.046	0.107	0.285	1
DGLαKO_MD	P31-34	L2/3	7	73	ODI	-0.072	0.052	-0.175	0.028	1
WT_noMD	P31-34	L4	9	86	ODI	-0.197	0.040	-0.274	-0.118	1
WT_MD	P31-34	L4	6	52	ODI	0.145	0.056	0.038	0.254	1
DGLαKO_MD	P31-34	L4	7	67	ODI	-0.072	0.047	-0.163	0.021	1
WT_noMD	P31-34	L5	9	150	ODI	-0.095	0.028	-0.149	-0.039	1
WT_MD	P31-34	L5	4	86	ODI	0.243	0.044	0.156	0.327	1
DGLαKO_MD	P31-34	L5	7	97	ODI	0.030	0.038	-0.044	0.108	1
WT_noMD	P17	L2/3	6	121	ODI	-0.139	0.030	-0.194	-0.081	2
WT_MD	P17	L2/3	5	94	ODI	-0.079	0.042	-0.158	0.004	2
DGLαKO_MD	P17	L2/3	6	163	ODI	-0.020	0.029	-0.074	0.039	2
WT_noMD	P17	L4	6	86	ODI	-0.140	0.041	-0.221	-0.059	2
WT_MD	P17	L4	5	76	ODI	-0.085	0.047	-0.177	0.007	2
DGLαKO_MD	P17	L4	6	97	ODI	-0.110	0.033	-0.174	-0.044	2
WT_noMD	P17	L5	6	183	ODI	-0.039	0.024	-0.089	0.009	2
WT_MD	P17	L5	5	174	ODI	-0.024	0.035	-0.089	0.046	2
DGLαKO_MD	P17	L5	6	209	ODI	-0.068	0.027	-0.121	-0.015	2
WT_noMD	P21	L2/3	5	99	ODI	-0.109	0.030	-0.168	-0.050	2
WT_MD	P21	L2/3	8	187	ODI	0.096	0.028	0.042	0.150	2
DGLαKO_MD	P21	L2/3	6	140	ODI	0.100	0.036	0.027	0.169	2
WT_noMD	P21	L4	5	86	ODI	-0.099	0.037	-0.172	-0.028	2
WT_MD	P21	L4	8	145	ODI	-0.013	0.033	-0.077	0.053	2
DGLαKO_MD	P21	L4	6	105	ODI	0.132	0.042	0.049	0.214	2
WT_noMD	P21	L5	5	157	ODI	0.022	0.029	-0.033	0.079	2
WT_MD	P21	L5	8	255	ODI	0.250	0.031	0.189	0.309	2
DGLαKO_MD	P21	L5	6	189	ODI	0.166	0.031	0.105	0.225	2
WT	P34-36	L2/3	8	60	Angle difference (degree)	27.5	3.1	21.9	34.1	2
WT	P34-36	L4	8	50	Angle difference (degree)	29.8	4.0	22.7	38.2	2
WT	P34-36	L5	8	52	Angle difference (degree)	33.7	4.0	26.2	41.8	2
DGLαKO	P34-36	L2/3	8	51	Angle difference (degree)	39.9	3.9	32.6	47.6	2
DGLαKO	P34-36	L4	8	61	Angle difference (degree)	36.6	3.2	30.7	43.3	2
DGLαKO	P34-36	L5	8	68	Angle difference (degree)	36.4	3.2	30.1	42.8	2
WT	P16-18	L2/3	4	28	mIPSC freq (Hz)	3.795	0.297	3.293	4.457	4
DGLαKO	P16-18	L2/3	4	31	mIPSC freq (Hz)	5.183	0.274	4.655	5.711	4
WT	P20-22	L2/3	3	17	mIPSC freq (Hz)	5.076	0.318	4.425	5.639	4
DGLαKO	P20-22	L2/3	3	17	mIPSC freq (Hz)	4.940	0.222	4.518	5.361	4
WT	P25-27	L2/3	5	16	mIPSC freq (Hz)	7.648	0.402	6.808	8.357	4
DGLαKO	P25-27	L2/3	4	13	mIPSC freq (Hz)	6.057	0.411	5.343	6.880	4
WT	P16-18	L4	3	25	mIPSC freq (Hz)	1.645	0.088	1.492	1.826	4
DGLαKO	P16-18	L4	3	25	mIPSC freq (Hz)	2.311	0.159	2.028	2.648	4
WT	P20-22	L4	5	23	mIPSC freq (Hz)	3.673	0.259	3.198	4.194	4
DGLαKO	P20-22	L4	4	16	mIPSC freq (Hz)	4.864	0.396	4.127	5.607	4
WT	P25-27	L4	2	21	mIPSC freq (Hz)	4.800	0.259	4.349	5.342	4
DGLαKO	P25-27	L4	4	14	mIPSC freq (Hz)	4.451	0.305	3.910	5.068	4
WT	P16-18	L2/3	4	28	mIPSC amplitude (pA)	18.503	0.724	17.176	19.914	4
DGLαKO	P16-18	L2/3	4	31	mIPSC amplitude (pA)	19.183	0.697	17.913	20.611	4
WT	P20-22	L2/3	3	17	mIPSC amplitude (pA)	19.601	0.837	18.159	21.422	4
DGLαKO	P20-22	L2/3	3	17	mIPSC amplitude (pA)	20.015	0.821	18.477	21.531	4
WT	P25-27	L2/3	5	16	mIPSC amplitude (pA)	20.618	1.073	18.788	22.874	4
DGLαKO	P25-27	L2/3	4	13	mIPSC amplitude (pA)	20.363	0.699	18.891	21.531	4
WT	P16-18	L4	3	25	mIPSC amplitude (pA)	26.468	0.937	24.828	28.519	4
DGLαKO	P16-18	L4	3	25	mIPSC amplitude (pA)	27.561	1.116	25.762	30.124	4
WT	P20-22	L4	5	23	mIPSC amplitude (pA)	26.381	1.101	24.362	28.580	4
DGLαKO	P20-22	L4	4	16	mIPSC amplitude (pA)	27.591	1.186	25.198	29.622	4
WT	P25-27	L4	2	21	mIPSC amplitude (pA)	27.373	0.720	26.114	28.874	4
DGLαKO	P25-27	L4	4	14	mIPSC amplitude (pA)	27.758	1.827	24.733	31.747	4
DGLαKO_MD	P17	all	6	526	ODI	-0.060	0.017	-0.091	-0.027	4
DGLαKO_MD_DMCM	P17	all	6	473	ODI	-0.043	0.017	-0.076	-0.010	4
DGLαKO_MD_DMCM	P17	L2/3	6	96	ODI	-0.038	0.039	-0.112	0.040	4
DGLαKO_MD_DMCM	P17	L4	6	60	ODI	-0.106	0.045	-0.193	-0.018	4
DGLαKO_MD_DMCM	P17	L5	6	186	ODI	-0.002	0.027	-0.056	0.050	4
DGLαKO_MD	P21	all	6	482	ODI	0.127	0.017	0.089	0.166	4
DGLαKO_MD_DMCM	P21	all	6	619	ODI	0.060	0.015	0.030	0.091	4
DGLαKO_MD_DMCM	P21	L2/3	6	79	ODI	0.142	0.043	0.058	0.225	4
DGLαKO_MD_DMCM	P21	L4	6	91	ODI	-0.076	0.037	-0.151	-0.005	4
DGLαKO_MD_DMCM	P21	L5	6	266	ODI	0.109	0.023	0.066	0.156	4
DGLαKO_noMD_WIN	P32-33	all	5	498	ODI	-0.085	0.013	-0.112	-0.056	4
DGLαKO_noMD_WIN	P32-33	L2/3	5	81	ODI	-0.068	0.032	-0.128	-0.001	4
DGLαKO_noMD_WIN	P32-33	L4	5	66	ODI	-0.141	0.041	-0.214	-0.053	4
DGLαKO_noMD_WIN	P32-33	L5	5	203	ODI	-0.113	0.021	-0.154	-0.071	4
DGLαKO_MD_WIN	P31-34	all	6	589	ODI	0.078	0.017	0.046	0.110	4
DGLαKO_MD_WIN	P31-34	L2/3	6	133	ODI	0.064	0.037	-0.007	0.136	4
DGLαKO_MD_WIN	P31-34	L4	6	114	ODI	0.012	0.038	-0.062	0.086	4
DGLαKO_MD_WIN	P31-34	L5	6	201	ODI	0.078	0.029	0.021	0.134	4